Journal of Dental Sciences

Volume 21 | Issue 2 Article 22

2026

Effects of L-ascorbic acid as an additive for improving the physical properties and setting behavior of fabricated calcium silicate cement

Yun-Jeong Park

Hyeon Seo

Yo-Han Song

Weon-Young Choi

Yeong-Joon Park

Journal of Dental Sciences 21 (2026) 850–862

Available online at https://jds.ads.org.tw/journal/

Digital Commons

journal homepage: https://jds.ads.org.tw/journal/

Original Article

Effects of L-ascorbic acid as an additive for improving the physical properties and setting behavior of fabricated calcium silicate cement

Yun-Jeong Park, Hyeon Seo, Yo-Han Song, Weon-Young Choi, Alphonse Umugire, Heejoo Ryu, Ho-Jun Song, Yeong-Joon Park*

Department of Dental Materials and Hard-Tissue Biointerface Research Center, School of Dentistry, Chonnam National University, Gwangju, South Korea

Received 11 July 2025; Final revision received 31 August 2025
Available online 1 April 2026

KEYWORDS
Dental cements;
Ascorbic acid;
Compressive strength;
Biocompatibility

Abstract *Background/purpose:* Calcium silicate (CS) cement presents significant drawbacks, including prolonged setting time, handling difficulty, and susceptibility to washout during early setting stages. Given the molecular structure of L-ascorbic acid (AscA), we hypothesized that it could influence the setting characteristics of CS cement. AscA is an effective antioxidant and possesses wide therapeutic properties. This study investigated the effects of AscA addition on the properties of CS cement.

Materials and methods: CS cement clinkers were synthesized and pulverized by jet milling. After characterization of the synthesized CS cement, the composition having high percentage of tricalcium silicate phase and low free CaO content (lime saturation factor 98.19) was selected. Addition of ZrO_2 (20 wt%) to the jet-milled CS powder followed by $CaSO_4 \cdot {}^1/_2H_2O$ (5 wt%) addition, was done to fabricate CS cement. AscA was incorporated into the mixing solution at various concentrations. Setting time, flow, penetration resistance, compressive strength, washout resistance, and MTT cytocompatibility were evaluated.

Results: Adding AscA up to 0.05 % enhanced the cement's flowability compared to the AscA-free control. AscA concentration negatively correlated with both setting time ($P < 0.01$, $r = -0.963$) and washout volume ($P < 0.01$, $r = -0.957$); setting time positively correlated with washout volume ($P < 0.01$, $r = 0.889$). Higher AscA correlated with increased early compressive strengths. The AscA-containing groups showed enhanced cell viability compared to the AscA-free group.

Conclusion: Incorporating AscA into CS cement resulted in faster setting, greater washout

* Corresponding author. Department of Dental Materials and Hard-Tissue Biointerface Research Center, School of Dentistry, Chonnam National University, 77 Yongbong-ro, Buk-gu, Gwangju 61186, South Korea.
E-mail address: yjpark@jnu.ac.kr (Y.-J. Park).

https://doi.org/10.1016/j.jds.2025.08.047

resistance, and higher compressive strength. Incorporating AscA into CS cement formulations is a promising approach for developing advanced CS cement.

Introduction

Calcium silicate cement (CS cement), commonly known as 'mineral trioxide aggregate (MTA)', was developed by Torabinejad in 1993.[1] Based on Portland cement, dental CS cement includes radiopaque agents such as bismuth oxide or zirconium oxide. It is widely applied in endodontic treatments such as pulp capping, pulpotomy, apexification, perforation repair, management of root resorption, canal sealing, orthograde root filling, and retrograde root-end filling.[2] This wide usage stems from its excellent sealing ability, biocompatibility, antibacterial effects, and dentin bridge formation.[3] However, CS cement presents significant drawbacks, including prolonged setting time, handling difficulty, and susceptibility to washout during early setting stages.[2]

Initially introduced as a retrograde root-end filling material, the first commercial MTA product, ProRoot MTA (Dentsply Inc., Tulsa, OK, USA), led to the development of numerous other commercial products. The setting time of ProRoot MTA is relatively long and is a significant disadvantage for procedures such as pulp capping and retrograde root-end filling. Various approaches have been explored to address this issue. For example, several studies have focused on modifying the powder components by altering the composition ratio,[4] controlling particle size,[5] or incorporating various additives. These modifications (including hydration accelerators such as calcium chloride, citric acid, lactic acid, calcium gluconate, and carboxyl ether polymers, or excluding calcium sulfate) have been used to reduce setting time.[6] While these approaches enhance the setting speed, they may negatively impact physical properties such as flowability and strength, biological compatibility, and tissue regeneration. Therefore, further investigations are needed to overcome these challenges.

Given the molecular structure of L-ascorbic acid (AscA), which can form coordinate bonds or ionic interactions with alkaline earth metal ions owing to its enediol structure and multiple hydroxyl groups,[7,8] we hypothesized that it could influence the setting characteristics of CS cement. L-ascorbic acid (AscA), a water-soluble vitamin (vitamin C), is an effective antioxidant that alleviates oxidative stress and participates in biochemical reactions as an important cofactor for several enzymatic reactions, and electron donor.[9,] Moreover, AscA possesses a broad spectrum of therapeutic properties, including antimicrobial, antiviral, antiparasitic, and antifungal effects.[10,11] Importantly, studies demonstrate AscA's role in promoting osteogenic differentiation.[12] It enhances collagen type 1 formation by hydroxylating proline and lysine residues in pro-collagen,[12] which aids osteogenic stem cell development and improves $\alpha 2\beta 1$ integrin binding to collagen type 1, which is crucial for osteogenesis.[13] Therefore, CS cement containing AscA was synthesized, and its effects on the cement's physical properties and biocompatibility were evaluated.

This study involved synthesizing fast-setting CS cement powder and examining the impact of AscA in the mixing liquid on the cement's physical properties and biological compatibility. The key physical properties evaluated comprised setting time, flowability, compressive strength, penetration resistance, and washout resistance. A quantitative, objective, and reproducible method was developed for assessing the flowability, washout resistance, and setting speed of CS cement groups without and with AscA at varying concentrations.

Materials and methods

Fabrication of calcium silicate cement

Analytical grade $CaCO_3$, SiO_2, Al_2O_3, MgO, K_2CO_3, Na_2CO_3, $CaSO_4 \cdot {}^1/_2H_2O$ (orthorhombic form), and ZrO_2 were obtained from Sigma–Aldrich (St. Louis, MO, USA). Isopropanol was obtained from Merck (Darmstadt, Germany), and phosphate-buffered saline (PBS) from Gibco (Carlsbad, CA, USA). Raw materials, including $CaCO_3$, SiO_2, Al_2O_3, MgO, K_2CO_3, and Na_2CO_3, were blended to achieve a lime saturation factor (LSF) of 98 (Table 1). The mixture was ball-milled in alumina pots with zirconia balls and isopropanol for 6 h, dried at 80 °C for 24 h, formed into balls with minimal water, and dried again at 80 °C for additional 24 h.

The dried balls were heat-treated to produce CS cement clinker: heated up to 600 °C at a rate of 5 °C/min, held for 30 min, and then further raised to 1450 °C, and maintained for 15 min. After sintering, the clinker was cooled in the furnace to 1250 °C, then removed and rapidly cooled to room temperature using a stainless steel fan with internal water circulation and external air blow. The sintered clinker was ground using an alumina mortar and pestle, and further milled to a mean particle diameter of 3.051 μm using a vibration mill (WTVM, Woongbi Machinery Co., Ltd, Cheonan, Korea; 1200 rpm) and a jet mill (STJ-200, JS Tech, Sacheon, Korea; 0.7 MPa pressure and 1 kg/h feeding speed). In addition, 5 wt% of $CaSO_4$ hemihydrate was incorporated, and 20 wt% ZrO_2 (Sigma–Aldrich) was further added as a radiopacifying agent. This mixture was homogeneously blended and used as the CS cement control.

Evaluation of crystalline phases of the synthesized cement clinker

The crystalline phases of the synthesized CS cement clinker were identified using X-ray diffractometry (XRD; X'Pert PRO Multi-Purpose Diffractometer, PANalytical, Almelo, Netherlands). The analysis was performed using Cu Kα

Table 1 Formulation of raw materials for dental calcium silicate cement clinker.

Compounds	$CaCO_3$	MgO	K_2CO_3	Na_2CO_3	SiO_2	Al_2O_3	Total
Weight %	76.413	2.786	1.525	0.256	13.063	5.956	100.000

radiation source (λ = 1.54056 Å) at 40 kV and 30 mA. Scanning was conducted over a 2θ range of 10°—70° at a rate of 1.8°/min. Diffraction patterns were interpreted using HighScore Plus software (PANalytical, Netherlands) with reference to the International Center for Diffraction Data (ICDD) database.

Particle size analysis and scanning electron microscopy

Particle size distribution was measured using a particle size analyzer (MasterSizer 2000, Malvern Instruments Ltd, Worcestershire, UK), with isopropyl alcohol as the dispersing medium. Particle sizes at 10 % (D_{10}) and 90 % (D_{90}) of the volume distribution were calculated. The morphology and elemental composition of the synthesized CS cement were observed using field emission scanning electron microscopy (FE-SEM; GeminiSEM 500, ZEISS Co., Oberkochen, Germany) coupled with energy dispersive spectrometry (EDS; Oxford Instruments, Abingdon, UK). Samples were prepared by compressing powders into a disk pellet (4 mm diameter) using a Teflon mold.

Moreover, the surface morphology of CS cement mixed with distilled water (DW) or 0.1 % AscA solution at a liquid/powder ratio of 0.55 was examined after 7 d. Mixtures were placed in a split Teflon mold (inner diameter 4 mm, thickness 1 mm) on a glass slide and demolded after 3 h. Samples were stored for 7 d at 37 °C under three conditions: 1) 100 % relative humidity (RH), 2) PBS (pH = 7.4; Merck), and 3) simulated body fluid (SBF) (pH = 6.8). Post-storage, samples were dried at 80 °C for 24 h, Pt-coated, and examined via FE-SEM (SU-70, Hitachi, Tokyo, Japan) operating at 15 kV.

Physical properties of CS cement types without or with AscA

Mixing procedure for CS cements

The AscA-containing solutions were prepared at concentrations of 0.01, 0.025, 0.05, 0.1, and 0.2 wt%, then filtered through a 0.22 μm syringe filter (Jet Biofiltration Co., Ltd., Guangzhou, China). To prepare the test samples, 0.3 g of CS cement powder was mixed with each solution for 1 min at a water/powder ratio (W/P ratio) of 0.55, under controlled conditions of 23 ± 1 °C and 50 ± 5 % RH. A sample of CS cement powder mixed with DW (0 wt% AscA) served as the control group.

Flowability

International organization for standardization (ISO) method

The flowability of the samples was assessed following ISO standard 6876.[14] A 0.05 mL portion of the mixed cement paste was loaded into a 1 mL syringe. After 3 min, the paste was dispensed onto a glass plate. Subsequently, a 40 mm × 40 mm glass plate (weighing ~20 g) was placed on top, followed by a 100 g weight. Ten minutes after initial mixing, the largest and smallest diameters of the spread specimen were measured using an image analyzer (I-Camscope, Sometech Co. Ltd., Seoul, Korea). Seven samples were tested per group.

Linear variable displacement transformer (LVDT) method

Fig. 1 depicts the schematic diagram of the flow-measuring test unit, consisting of a displacement-measuring digital gauge with a linear variable displacement transformer (LVDT). This flowability test method was developed to improve the discernibility of ISO standard 6876. A 0.05 mL portion of the mixed cement paste was loaded into a 1 mL syringe. After 60 s from the start of mixing, the mixture was dispensed onto a glass plate, and a cover glass was placed on top. After 90 s from the start of mixing, a 500 g load was applied. The change in height of the loading rod was measured up to 10 min after mixing. These measurements were digitized using a digimatic data logger connected to the LVDT of the digital gauge and recorded using ComPortMaster software (Withrobot Inc., Seoul, Korea). The reduction in specimen height, relative to its initial height, was calculated and expressed as a percentage of shortening. This experiment was replicated seven times.

Setting time

The setting time was determined following ISO standard 6876 (2012). The CS cement was mixed at 23 ± 1 °C and 60 ± 5 % RH. The mixture was then filled into a metal mold with a 10 mm diameter and 2 mm height dimensions, ensuring the surface was leveled to the mold's height. The mold-filled sample was placed inside a temperature and humidity controlled cabinet (37 ± 1 °C and 70 ± 5 % RH). The setting time was measured using a Gilmore needle (100 ± 0.5 g) with a flat-ended indenter (2 ± 0.1 mm diameter) inside a controlled cabinet. The needle was gently lowered vertically onto the sample, and the time point at which no indentation remained was recorded. This test was repeated for seven samples.

Washout resistance

The cement mixture was placed into a metal mold having an indent with 10 mm inner diameter and 2 mm depth. The mold was secured using a bisected fixture at the center of a polisher's rotating plate (300 rpm) (Phoenix Beta, Buehler Ltd., Dusseldorf, Germany). At 150 s after the start of

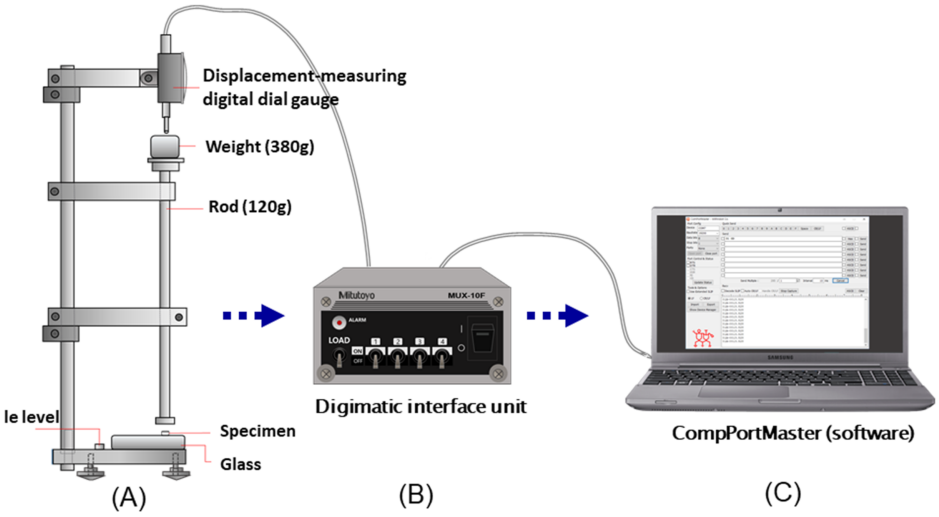

Figure 1 Schematic diagram of the flow measuring test unit consisting of a displacement measuring digital gauge with linear variable displacement transformer (A), a digimatic data logger (B), and Comportmaster software (C).

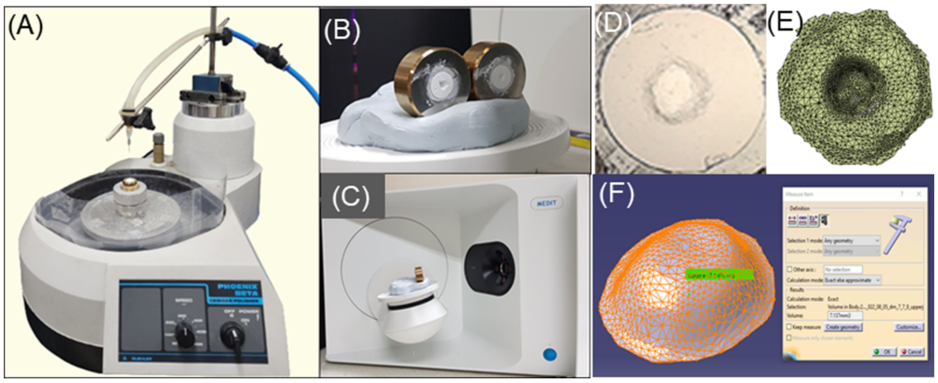

Figure 2 Washout resistance test setup: (A) water jet impinging onto a spinning sample surface (300 rpm) for 5 s. Water from a circulating water bath (60 mL/min, 37 °C) is sprayed through an 18 G needle, the tip of which is positioned 45 mm over the sample surface; (B) washed-out sample positioned on stage; (C) scanning with three-dimensional (3D) scanner; (D) optical image of the washed-out surface; (E) meshed standard for the exchange of product model data (STEP) file of scanned surface; (F) washout volume calculation with computer aided three-dimensional interactive application version 5 (Catia V5).

mixing, a water spray (60 mL/min, 18 G needle, 45 mm distance) was applied to the sample surface for 5 s.

The washed-out indented area was scanned using a 3D scanner (T710, Medit, Seoul, Korea) to generate a stereolithography (STL) file. The STL data were converted into a Standard for the exchange of product model data (STEP) file via FreeCAD (version 0.20, open-source software, available at https://www.freecad.org), and the washout volume was calculated using computer aided three-dimensional interactive application version 5 (Catia V5) (Dassault Systèmes Korea Corp., Incheon, Korea) (Fig. 2). This experiment was replicated three times.

Penetration resistance

To assess the hardening kinetics of freshly mixed cement, penetration resistance was measured using an automated device (Fig. 3). A cylindrical tip (2 mm diameter) attached to a digital force gauge (FGP-5, Nidec-Shimpo Co., Kyoto, Japan) was lowered to a 0.8 mm depth at 30 μm/s operated by a stepping motor using a LabVIEW program (National Instruments Corp., Austin, TX, USA). The cement mixture was placed in a metal mold (W 28 mm x D 5 mm x H 2 mm), and penetration resistance was measured at 3, 6, 9, 12, 15, 20, 30, 45, and 60 min post-mixing under 23 ± 1 °C and 60–70 % RH. The resistance force was read 20 times/s via a LabVIEW program. The resistance force was divided by the penetrating tip's cross-sectional area, and expressed in megapascals (MPa). Then, the data were plotted as a spline curve graph. Penetration resistance values were extracted from image graph over time using the Engauge digitizer software, an open-source digitizing tool developed by Mark Mitchell. The test was replicated five times, and the average times to reach 30, 40, 50, and 60 MPa resistance were calculated.

Compressive strength

Compressive strength was evaluated according to ISO 9917-1,[15] as no specific ISO standard exists for CS cement. The

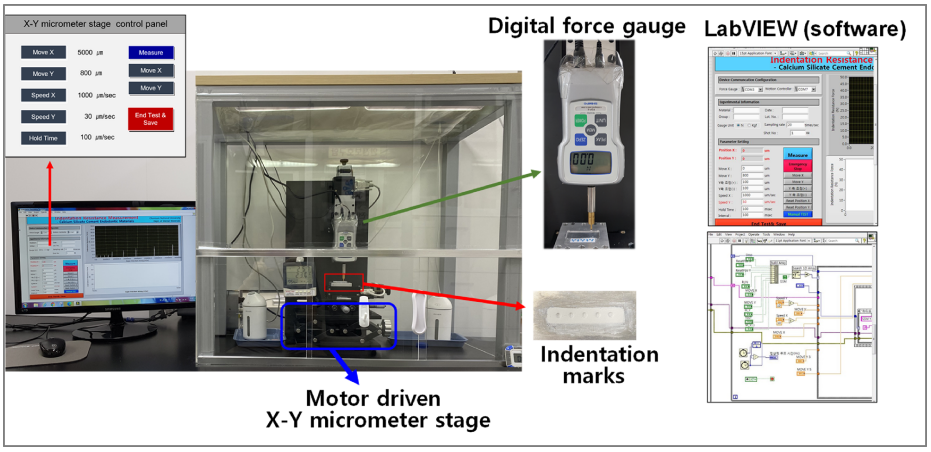

Figure 3 Penetration resistance measuring setup: automated micrometer stage control and data acquisition using LabVIEW.

mixed cement was packed into a split-ring Teflon mold (6.0 ± 0.1 mm height × 4.0 ± 0.1 mm ID), and excess was removed with a flat spatula. Specimens were placed in a 37 ± 1 °C, 100 % RH chamber for 3 h, then surfaces were finished using 400-grit SiC paper and demolded. Sets of seven specimens per group were stored at 37 ± 1 °C and 100 % RH for 1, 3, and 7 days. Compressive strength was measured using a universal testing machine (Instron 4302, Instron Ltd., High Wycombe, UK) at a 1.0 mm/min crosshead speed.

Biocompatibility

Mouse fibroblast-like cells (L-929; National Collection of Type Cultures [NCTC] clone 929) were seeded at 1×10^5 cells/well in a 96-well plate and incubated for 24 ± 1 h at 37 ± 1 °C under 5 % CO2. Cells were cultured in RPMI complete medium, prepared by supplementing minimum essential medium (DMEM; Gibco, Thermo Fisher Scientific, Waltham, MA, USA, #11995) with 5 % fetal bovine serum (FBS; Gibco, #16140) and 1 % penicillin/streptomycin (Gibco, #15140).

CS cement powder was mixed with DW at a W/P ratio of 0.55, molded into a split Teflon mold (diameter 10 mm, height 2 mm), and set for 24 h at 37 ± 1 °C and 99 % RH. The hardened specimens were demolded, sterilized under ultraviolet (UV) light for 30 min on each side, and immersed in 1 mL of RPMI complete medium for 24 h at 37 ± 1 °C. The supernatant, obtained by centrifuging the leachate to remove particulates, was serially diluted to 100 %, 50 %, 25 %, and 12.5 % using RPMI complete medium.

Cytotoxicity was assessed using the MTT assay following ISO standard 10993-5.[16] After 24 h of cell culture, the media were removed and replaced with 100 μL of the diluted extracts, followed by a 24 h incubation. Control wells received fresh RPMI complete medium. After incubation, extracts were removed, and 100 μL of MTT solution (0.5 mg/mL concentration of 3-(4,5-dimethylthiazol-2-yl)-2,5-diphenyltetrazolium bromide, Sigma–Aldrich, #M2128) was added to each well and incubated for 4 h at 37 ± 1 °C. The MTT solution was discarded, and 100 μL of dimethyl sulfoxide (DMSO; Sigma–Aldrich) was added to dissolve formazan crystals, followed by 15 min incubation at room temperature. Absorbance was measured at 570 nm using a microplate reader (Sunrise™ microplate reader, Tecan Group Ltd., Männedorf, Switzerland), and cell viability was expressed as a percentage relative to the control. The test was replicated five times.

Statistical analysis

The data for flowability, setting time, and washout resistance were analyzed using the Kruskal–Wallis test followed by Tukey's post hoc test for multiple comparisons in SPSS software (version 26.0, IBM Software, Armonk, NY, USA). Compressive strength was evaluated by two-way analysis of variance (ANOVA), and Tukey's multiple comparison tests were performed. Statistical significance was set at $P < 0.05$.

Results

Characterization of the fabricated CS cement

X-ray diffraction analysis

Fig. 4 presents the XRD patterns of the synthesized CS clinker powder (A), CS cement powder (B), and set CS cement after hydration by mixing with either DW (C) or 0.1 wt% AscA solution (D) and storing at 37 °C and 100 % RH for 7 d.

The XRD pattern of the CS clinker powder exhibited characteristic peaks corresponding to tricalcium silicate at $2\theta = 34.39$, 32.24, 32.65, and 29.48 (ICDD 00-042-0551), dicalcium silicate at $2\theta = 32.20$, 32.11, 32.65, 34.39, and 41.26) (ICDD 00-033-0302), and tricalcium aluminate at $2\theta = 33.33$, 33.11, and 33.01) (ICDD 00-038-1429) (Fig. 4A). These phases match the expected clinker composition, confirming successful synthesis.[17]

Following milling and adding 5 wt% $CaSO_4$ hemihydrate and 20 wt% ZrO_2, the XRD pattern of the CS cement powder showed additional peaks attributable to these additives. The newly emerged peaks, corresponding to $CaSO_4$ hemihydrate (ICDD 00-014-0453) and ZrO_2 (ICDD 00-037-1484), alongside the existing tricalcium silicate, dicalcium silicate, and tricalcium aluminate peaks (Figs. 4B),[17] indicate effective incorporation of these materials, altering the mineralogical composition and potentially enhancing hydration performance.

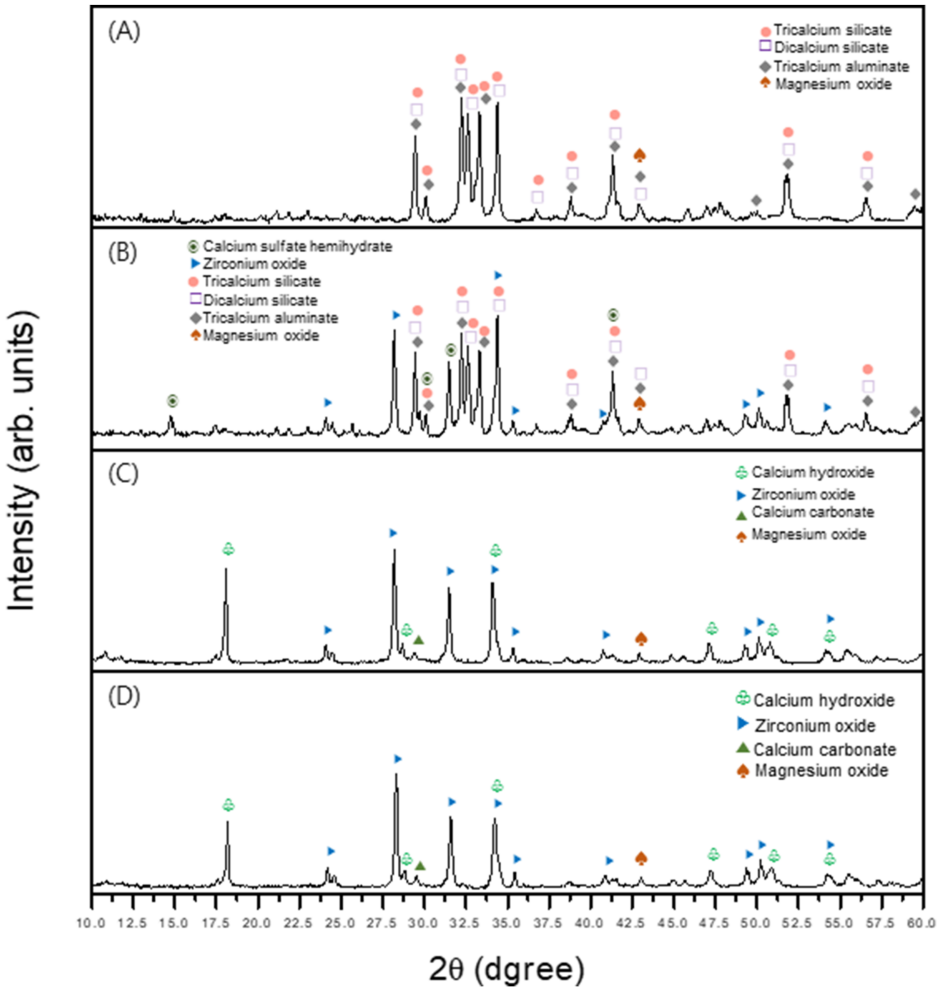

Figure 4 X-ray diffraction (XRD) patterns of calcium silicate (CS) clinker powder, CS cement powder, and CS cement set at 37 °C and 100 % relative humidity for 7 days: (A) CS clinker powder, (B) CS cement powder, (C) hydrated CS cement mixed with distilled water, and (D) hydrated CS cement mixed with 0.1 % L-ascorbic acid (AscA) solution. *Symbols*: ●, Tricalcium silicate; □, Dicalcium silicate; ◆, Tricalcium aluminate; ◉, Calcium sulfate hemihydrate; ▲, Calcium carbonate; ♧, Calcium hydroxide; ▶, Zirconium oxide; ♠, Magnesium oxide.

The XRD patterns of the 7-day hydrated CS cement, mixed with either DW or 0.1 wt% AscA solution, are shown in Fig. 4C and D, respectively. Both patterns revealed peaks of calcium hydroxide at $2\theta = 34.13$, 18.07, and 47.10 (ICDD 00-044-1481) and $CaCO_3$ at $2\theta = 29.42$ and 35.94 (ICDD 00-005-0586), along with zirconium oxide phases (Fig. 4C and D).

Particle size analysis and scanning electron microscopy

Vibration milling of the ball-milled CS powder reduced its average particle size to 59.122 μm, with a particle size distribution of 2.345 μm for D_{10} and 162.194 μm for D_{90} (Fig. 5A). Further refinement by jet milling decreased the average particle size to 3.051 μm, with D_{10} and D_{90} values of 0.552 μm and 6.397 μm, respectively (Fig. 5B).

The SEM image and EDX spectra with elemental concentration of the CS powder processed by vibration and jet milling are shown in Fig. 6.

The SEM images of hardened CS cement surfaces stored under various conditions are shown in Fig. 7. Specimens cured for 7 days after mixing with either DW or 0.1 % AscA solution displayed small, uniformly sized granular structures (Fig. 7A and B). Conversely, CS cement mixed with 0.1 % AscA and cured for 7 days in PBS exhibited acicular, spherule-like crystalline structures (Fig. 7C), indicating significant interaction between the cement and PBS.[18] Samples mixed with 0.1 % AscA and cured in SBF for 7 days (Fig. 7D) revealed a highly complex microstructure. Petal-like crystals (rectangle box 'A',[19]), were overlaid by spherical calcium phosphate clusters (box 'B',[20]), suggesting a dual-phase process wherein SBF promoted both hydration of calcium silicate phases and calcium phosphate deposition. The petal-like structures increase surface area, potentially promoting further mineralization, while the calcium phosphate clusters suggest bioactivity, indicating suitability for applications such as dentin bridge formation and bone repair.[20,21]

Flowability

Using ISO and LVDT methods, CS cement mixed with 0.05 % AscA solution exhibited the highest flowability. Flowability

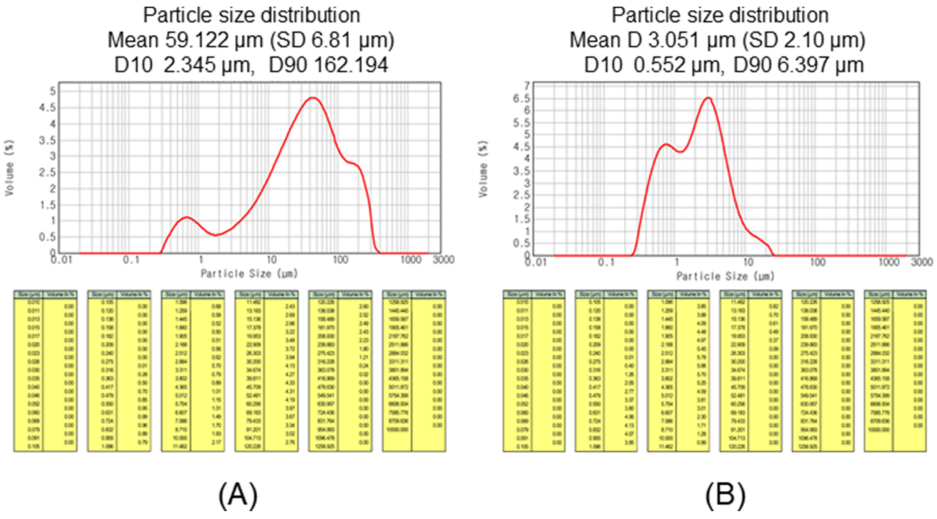

Figure 5 Particle size distribution of synthesized calcium silicate powder after (A) vibration and (B) jet milling.

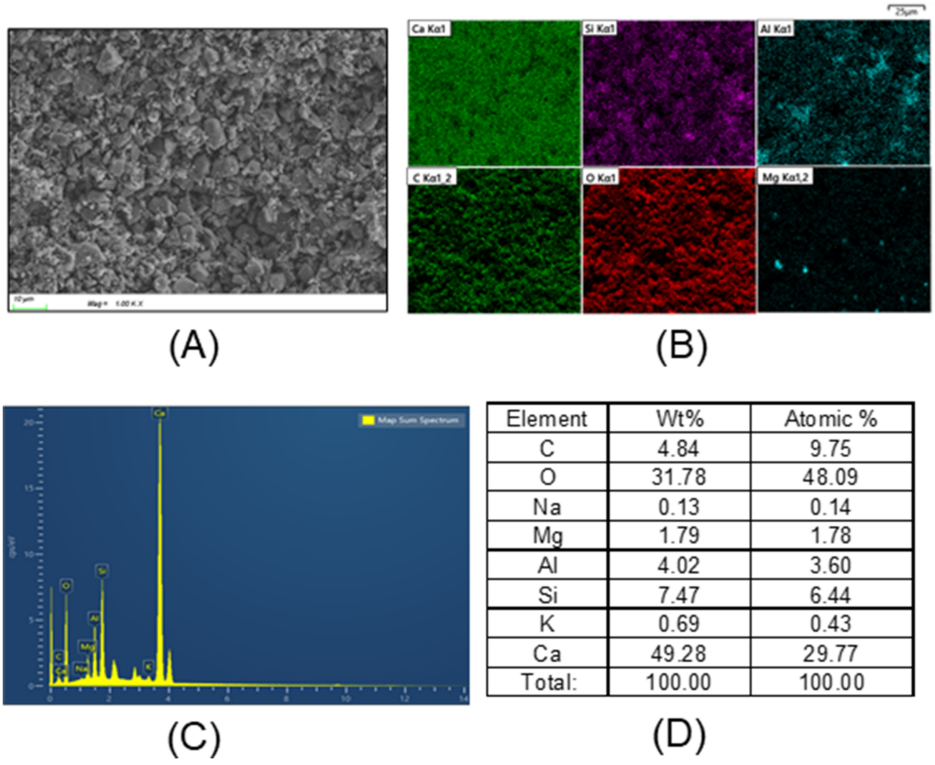

Element	Wt%	Atomic %
C	4.84	9.75
O	31.78	48.09
Na	0.13	0.14
Mg	1.79	1.78
Al	4.02	3.60
Si	7.47	6.44
K	0.69	0.43
Ca	49.28	29.77
Total:	100.00	100.00

Figure 6 Scanning electron microscopy (SEM) image at 1000× magnification (A) and energy dispersive x-ray spectroscopy (EDX) elemental analysis (B—D) of calcium silicate (CS) powder ground by vibration and jet milling.

increases with AscA concentration up to 0.05 % when the ISO method is used. However, the flowability decreased significantly beyond this point ($P < 0.05$), decreasing from 6.96 mm in the 0.05 % AscA group to 5.89 mm in the 0.2 % AscA group (Fig. 8, left vertical axis). The initial increase is likely due to the plasticizing effect of AscA concentration, whereas the subsequent decrease may reflect accelerated reaction product formation at higher concentrations.

Similarly, the LVDT method showed that AscA concentrations up to 0.05 % significantly improved flowability ($P < 0.05$). Sample height reduction was 51.23 % for the 0.05 % AscA group compared to 49.76 % for the 0 % group (Fig. 8, right vertical axis). Beyond 0.05 % AscA, flowability decreased significantly, with sample height reduction values dropping from 51.23 % (0.05 % AscA) to 45.15 % (0.1 % AscA) and 27.40 % (0.2 % AscA) (Fig. 8, right vertical axis).

Setting time

The setting times of the test samples, measured using the ISO method, are presented in Fig. 9 (pink color). When the

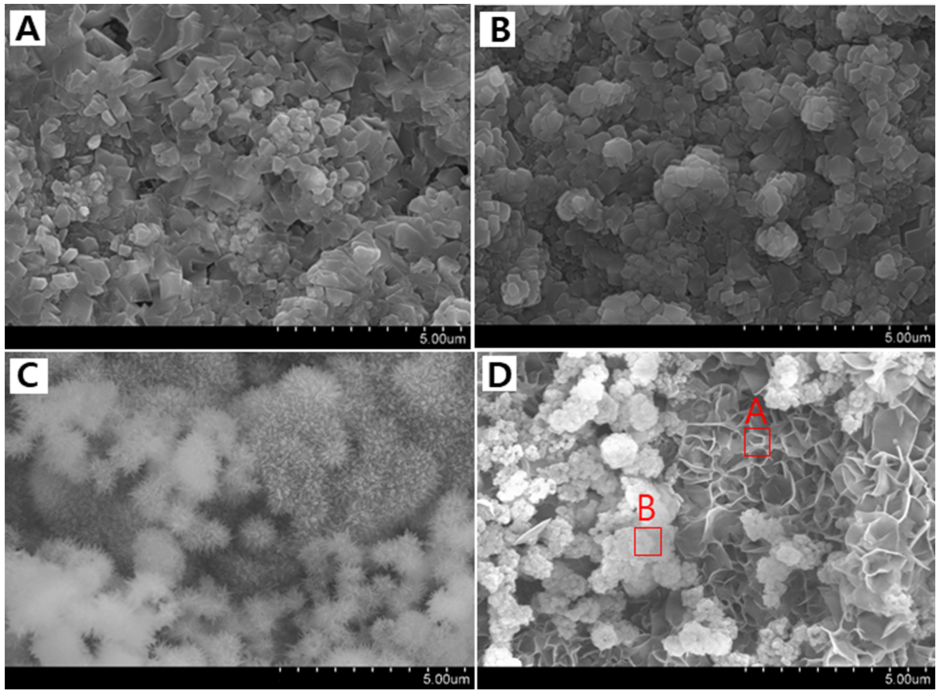

Figure 7 Scanning electron microscopy (SEM) images of calcium silicate (CS) cement hardened at 37 °C and 100 % relative humidity for 7 days (10,000× magnification): (A) CS cement mixed with distilled water without immersion; (B) CS cement mixed with 0.1 % L-ascorbic acid (AscA) solution without immersion; (C) CS cement mixed with 0.1 % AscA solution and stored in phosphate-buffered saline; (D) CS cement mixed with 0.1 % AscA solution and stored in simulated body fluid.

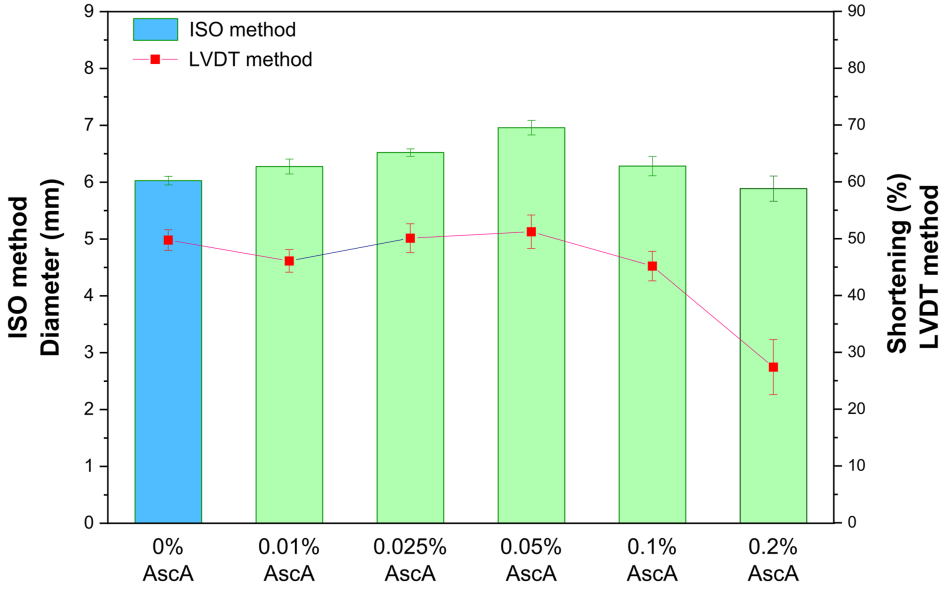

Figure 8 The results of the flowability test determined by the International organization for standardization (ISO) method and linear variable displacement transformer (LVDT) method. * Different uppercase letters (within ISO method) and different lower letters (within LVDT method) indicate significant differences between groups at $P = 0.05$, with n = 7 replicates for each group.

AscA concentration in the mixing solution exceeded 0.025 %, the AscA-containing groups exhibited significantly shorter setting times compared to the AscA-free group (25.27 ± 0.72 min) ($P < 0.05$). The 0.2 % AscA group demonstrated the shortest setting time (9.75 ± 0.77 min), significantly lower than that of the other groups ($P < 0.05$).

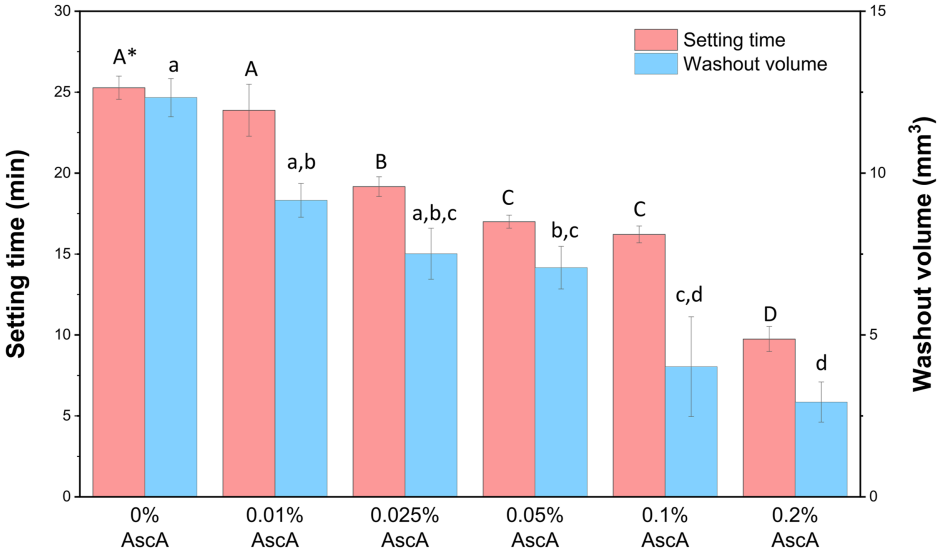

Figure 9 Mean and standard deviation of setting time (min; n = 7) and washout volume (mm^3; n = 3) for calcium silicate cement samples. *Different uppercase (setting time) and lowercase letters (washout resistance) indicate significant differences between groups at $P = 0.05$.

Table 2 Mean and standard deviation of the washed-out volume (mm^3) of the calcium silicate cement samples, with n = 3 replicates for each group.

Groups	Concentration of AscA in mixing liquid (wt%)					
	0 %	0.01 %	0.025 %	0.05 %	0.1 %	0.2 %
Washed-out volume (mm^3)	12.33^{aa} (0.59)	$9.16^{a,b}$ (0.52)	$7.51^{a,b,c}$ (0.79)	$7.08^{b,c}$ (0.66)	$4.02^{c,d}$ (1.54)	2.93^{d} (0.62)

[a] Different small lowercase letters indicate significant differences between groups at $P = 0.05$.

A strong negative correlation was observed between AscA concentration and setting time ($P < 0.01$, r = −0.963).

Washout resistance

The washout volumes measured under the conditions described in section 2.3 are demonstrated in Table 2 and Fig. 9. All AscA-containing groups exhibited lower washout volumes than the control. The 0.2 % AscA group showed the most significant resistance to washout. Increasing AscA concentrations correlated with reduced washout volume ($P < 0.01$, r = −0.957). Furthermore, AscA concentration negatively correlated with both setting time ($P < 0.01$, r = −0.963) and washout volume ($P < 0.01$, r = −0.957); setting time positively correlated with washout volume ($P < 0.01$, r = 0.889).

Penetration resistance

Fig. 10 presents the average resistance values (MPa) of the mixed CS cement samples against 0.8 mm penetration plotted over time after mixing.

As summarized in Table 3, the average time required to reach the specific penetration resistance (MPa) values decreased with increasing AscA concentration in the mixing solution, except for the 0.01 % AscA group.

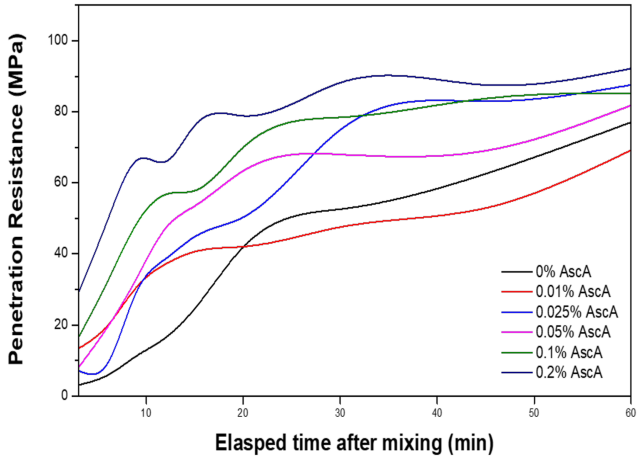

Figure 10 Average resistance values (MPa) of mixed calcium silicate cement samples against 0.8 mm penetration over elapsed time after mixing, with n = 5 replicates for each group.

Compressive strength

The compressive strengths of the CS cements increased with aging (Fig. 11). At 7 days, the highest strength values were observed across all groups (except the 0.1 % AscA group) ($P < 0.05$), with compressive strengths converging across groups by this point ($P > 0.05$).

Table 3 Average elapsed time (min) for mixed calcium silicate cement to reach penetration resistance values of 30, 40, 50, and 60 MPa (at 0.8 mm penetration), with n = 5 replicates for each group.

Penetration resistance (MPa)	Concentration of AscA in mixing liquid (wt.%)					
	0 (Control)	0.01	0.025	0.05	0.1	0.2
30	14.3	6.1	6.5	5.7	2.9	0.2
40	17.3	11.9	10.2	7.8	4.6	1.7
50	22.7	36.3	17.7	10.6	6.7	3.3
60	40.9	52.4	22.7	16.0	14.1	4.8

groups exhibited favorable cell viability, surpassing 100 % relative to the control (AscA-free) group. Exceptions were noted under specific conditions in the 0.05 %/50 %, 0.1 %/100 %, 0.2 %/50 %, and 0.2 %/100 % groups (AscA %/extract dilution %) (Fig. 12).

Discussion

The XRD pattern of the CS clinker powder synthesized in this study showed characteristic peaks corresponding to tricalcium silicate, dicalcium silicate, and tricalcium aluminate (Fig. 4A), which confirmed the successful synthesis.[17] Tricalcium silicate and dicalcium silicate are critical for hydration, with tricalcium silicate contributing to early setting through rapid hydration and dicalcium silicate promoting long-term strength through slower hydration. Because having a large portion of tricalcium silicate rather than dicalcium silicate is beneficial for getting early

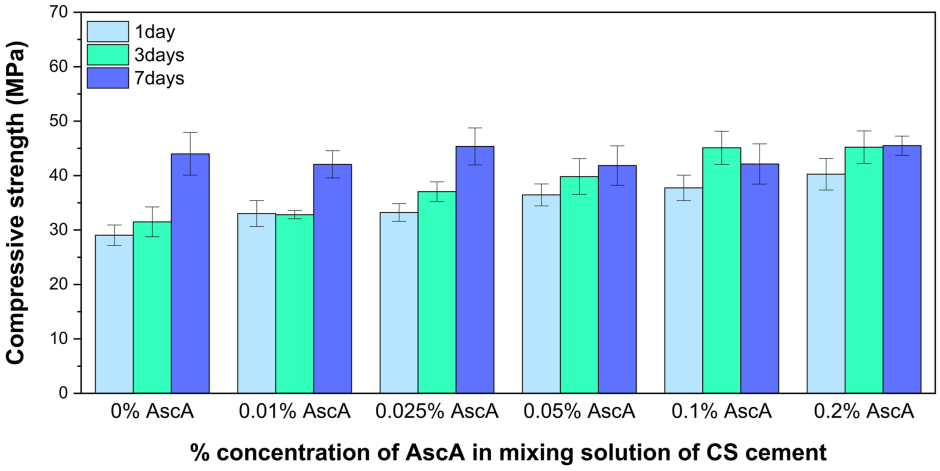

Figure 11 Mean and standard deviation values of compressive strength (MPa) of calcium silicate cements with varying L-ascorbic acid (AscA) concentrations (%) in the mixing solution and across different aging times, with n = 7 replicates for each group.

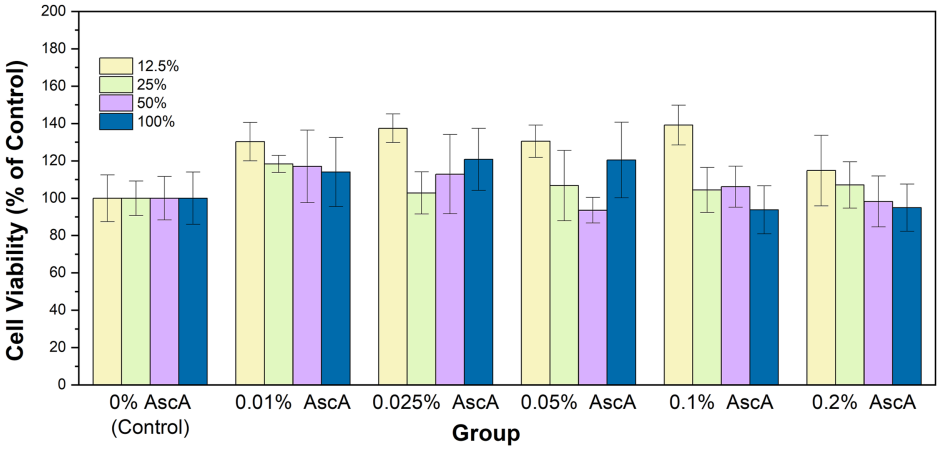

Figure 12 Cell viability of calcium silicate cements. The cell viability (% viability compared to the control group) is shown according to L-ascorbic acid (AscA) concentration in the mixing solution and elution extract dilutions. Statistical significance at $P < 0.05$ (Two-way ANOVA), with n = 5 replicates for each group.

Biocompatibility

The biocompatibility of CS cement extracts at concentrations of 12.5 %, 25 %, 50 %, and 100 % was assessed across five AscA-containing groups (0.01 %–0.2 % AscA). Most

setting,[22] the composition of this study was blended to achieve a lime saturation factor (LSF) of 98, which is higher than that of ordinary CS cement.

In the XRD patterns of the 7-day hydrated CS cement, mixed with either DW or 0.1 wt% AscA solution (Fig. 4C and D, respectively), both patterns revealed peaks of calcium hydroxide and $CaCO_3$, along with zirconium oxide phases. However, tricalcium silicate and dicalcium silicate peaks were absent in the 7-d hydrated samples, whereas Voicu et al. reported only a reduction in these peaks.[23] This observation indicates that both phases underwent complete or near-complete hydration, rendering them undetectable in the hydrated specimen. The absence of CS hydrate peaks can be attributed to its low crystallinity. The inclusion of AscA in the mixing solution did not significantly alter peak intensities or positions. However, further quantitative studies are warranted to elucidate its potential influence on hydration kinetics and microstructural development.

In this study, we prepared fine particles with the average size of 3.051 μm using jet-milling (Fig. 5B). This particle size reduction is critical, as finer particles increase specific surface area, thereby enhancing powder reactivity and accelerating setting rates.[24] Post-jet-milling, the particles exhibited a predominantly spherical morphology (Fig. 6A), which favors easy mixing and efficient packing for material performance. Elemental mapping by EDS (Fig. 6B—D) confirmed the homogeneous distribution of the constituent elements throughout the sample, which is critical for ensuring structural uniformity and consistent mechanical properties in the CS cement.

In this study, we evaluated the flow property using two different methods. The ISO 6876 method, initially designed for dental root canal sealers, presents challenges when applied to CS cement.[14,25] Manual centering of the glass plate is difficult, and repeatedly measuring the minimum and maximum diameters of the compressed disc with calipers until the diameters are within 1 mm of each other, proves to be complex and far from straightforward introducing substantial user-related errors. Therefore, in this study, a novel flowability measurement method using an LVDT was developed. The LVDT, which measures linear displacement digitally, produces continuous, real-time data,[26] making capturing precise flowability changes easier. Compared with ISO 6876, the LVDT method more clearly reflects changes in flowability. In summary, the consistent trends observed in both methods indicate support for LVDT as a promising alternative for assessing CS cement flowability.

As shown in Fig. 8, the flowability of CS cement, measured by both the ISO and LVDT methods, clearly depended on the concentration of AscA in the mixing solution. A paste with good flowability ensures a comfortable working environment for clinicians and it is crucial for the successful penetration of CS cement into every narrow root canal spaces.[2,27] Therefore, flowability is a key factor for successful endodontic treatment. However, while high flowability is desirable for procedures like root canal sealing,[28] other clinical situations, such as retrograde fillings or cement base applications, require sufficient viscosity to maintain the cement's stability at the applied site. Therefore, the findings of this experiment provide critical information for optimizing CS cement formulations for different applications by balancing flowability and mechanical strength. This study demonstrated that the flowability of CS cement could be effectively controlled by incorporating small amounts of AscA into the mixing solution, with the degree of flowability adjustable by varying AscA concentrations.

A prolonged setting time is a significant drawback in the clinical use of CS cement.[29] Since setting time is heavily influenced by particle size,[30] the mean particle size of 3.051 μm for the jet-milled CS clinker powder indicates a smaller particle size than commercial MTA products.[29] Consequently, the average setting time of the control group in this study (25.27 ± 0.72 min) was shorter than that of many commercial products.[2,20,29] While shorter setting times are advantageous in the oral environment, reducing treatment time and minimizing contamination risks, overly rapid setting can impair workability.[2,31] Therefore, achieving an optimal setting time is critical. This study found that incorporating AscA into the mixing solution effectively reduced the CS cement's setting time (Fig. 9). Adding AscA up to 0.05 % enhanced the cement's flowability compared to the AscA-free control (Fig. 8). Improved flowability facilitates better penetration into the complex root canal geometries, promoting effective sealing and potentially reducing risks of leakage or reinfection.[2,32] This method of lowering setting time using AscA is especially valuable for endodontic applications, where high flowability combined with appropriate setting time enhances clinical utility.[2,5] Further research is warranted to elucidate the mechanisms by which AscA modifies the physical properties of CS cement.

Disintegration of cement paste can compromise sealing and trigger inflammatory responses. Slow-setting materials are particularly vulnerable to washout when exposed to tissue fluids, blood, or irrigation. Therefore, enhancing washout resistance is crucial for successful root canal treatments, particularly for cement types with extended setting times.[6] Various methods have been employed to assess CS cement washout resistance, including immersion and visual scoring by multiple observers,[33] solution spraying followed by visual inspection,[34] weight-based calculations of washed and retained material,[35] and adaptations from concrete industry standards such as CRD-C 661-06 specification.[36] However, there remains a need for more objective, quantitative approaches. In response, a novel test method was developed based on the 'jet impingement' method, originally used to evaluate cell adhesion strength. In our adapted method, a fluid jet impacts the specimen under controlled conditions,[37,38] and the washed-away portion is captured via 3D scanning. The washout volume was then quantified using Catia V5 3D modeling software, offering a highly visual, quantitative, and objective assessment.

The ISO flowability results showed that all experimental groups, except the 0.2 % AscA group, exhibited higher flowability than the control. Despite this increased flowability, AscA-containing groups demonstrated superior washout resistance. This combination of high flowability and low washout volume is particularly advantageous for root canal sealing procedures, where both properties are critical for clinical success.

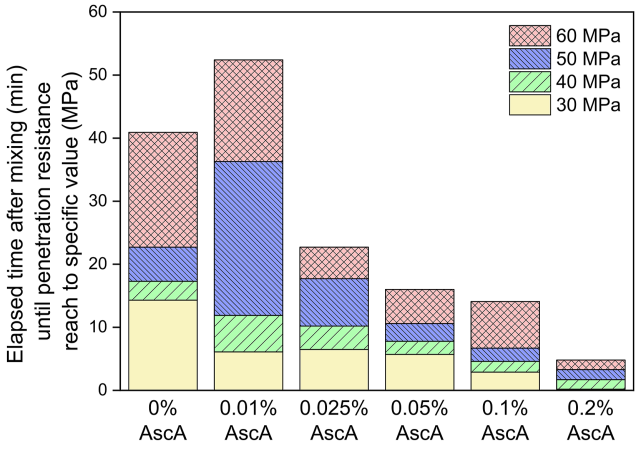

Figure 13 Average elapsed time (min) for mixed calcium silicate cement to reach the penetration resistance values of 30, 40, 50, and 60 MPa at various L-ascorbic acid (AscA) concentration groups, with n = 5 replicates for each group.

In the result of penetration resistance test (Fig. 10, Table 3), the average time required to reach the specific penetration resistance (MPa) values decreased with increasing AscA concentration in the mixing solution, except for the 0.01 % AscA group. This trend is more clearly illustrated in Fig. 13, illustrating the average elapsed time (min) needed to achieve resistance values of 30, 40, 50, and 60 MPa across different AscA concentration groups. A reduction in the time required to develop penetration resistance indicates faster material hardening, a crucial factor in clinical procedures requiring rapid setting, such as pulp capping, perforation repair, and retrograde filling.[39] Faster hardening improves procedural efficiency and enhances the overall clinical outcome. The penetration resistance trends (Table 3, Figs. 10 and 13) were consistent with the setting time results (Fig. 9) regarding the effect of AscA addition. This agreement across different assessment methods reinforces the notion that AscA enhances the hardening behavior of CS cements.

This study introduced a novel method for evaluating the hardening behavior of CS cement during setting, utilizing a digital force gauge. Data acquisition, test automation, and instrument control were managed using the LabVIEW program. Unlike the ISO method employing a Gilmore needle, this mechanical approach reduces operator skill dependence and minimizes variability. Results, expressed as the time required to reach a specified penetration resistance value (MPa), indicate that the gel-like mixture progressively hardens. Faster attainment of penetration resistance reflects a quicker setting process. Our findings revealed a consistent trend of accelerated setting with AscA addition, as shown by penetration resistance and setting time measurements.

Higher AscA correlated with increased early compressive strengths at 1 d and 3 d. This enhancement is crucial for perforation repairs in root furcation areas, where materials must withstand occlusal forces. Compressive strength reflects the degree of hydration and material setting in hydraulic cements.[6] These results reflect AscA's potential to improve the mechanical properties of CS cement, enhancing its clinical performance.

The biocompatibility test results (Fig. 12) indicated a promising trend toward enhanced biocompatibility across varying extract and AscA concentrations. Most AscA-containing groups showed no cytotoxicity, with cell viability consistently above 100 % compared to the control. According to ISO 10993 standards, which define biocompatibility as cell viability greater than 70 %, all tested samples met the criteria.[16,40] A cytotoxicity study by Golonka et al. showed that ascorbic acid concentrations above 2.5 % exhibited cytotoxic effects on L929 fibroblasts.[10] Nonetheless, the general trend of increased cell viability following AscA supplementation observed in our study supports its potential as a valuable additive in CS cement formulations, contributing to improved biocompatibility and physical properties for clinical use. Further research into the cellular mechanisms and long-term effects of AscA supplementation is needed to fully understand its benefits.

Incorporating AscA into CS cement substantially improved its physical properties, including faster setting time, enhanced washout resistance, and increased compressive strength, all critical for clinical use in humid biological environments. The inclusion of AscA presents a promising strategy for manufacturing advanced CS cements.

Declaration of competing interest

The authors declare no conflict of interest.

Acknowledgments

The authors acknowledge the financial support from the National Research Foundation of Korea (NRF) grant funded by the Korean government (MSIT) (No. 2019R1A5A2027521 and No.2019R1A2C1009377).

References

1. Torabinejad M, Watson TF, Pitt Ford TR. Sealing ability of a mineral trioxide aggregate when used as a root end filling material. *J Endod* 1993;19:591–5.
2. Camilleri J. *Endodontic materials in clinical practice*. Hoboken: Wiley, 2021.
3. Kim B, Lee YH, Kim IH, et al. Biocompatibility and mineralization potential of new calcium silicate cements. *J Dent Sci* 2023;18:1189–98.
4. Lim J, Guk JG, Singh B, Hwang YC, Song SJ, Kim HS. Investigation on hydration process and biocompatibility of calcium silicate-based experimental Portland cements. *J Korean Ceram Soc* 2019;56:403–11.
5. Ha WN, Nicholson T, Kahler B, Walsh LJ. Methodologies for measuring the setting times of mineral trioxide aggregate and Portland cement products used in dentistry. *Acta Biomater Odontol Scand* 2016;2:25–30.
6. Tilakchand M, Pandey P, Shetty P, Naik B, Shetti S. The comparative evaluation of various additives on setting time and compressive strength of MTA plus: an in vitro study. *Endod* 2021;33:36–42.

7. Davies MB. Reactions of L-ascorbic acid with transition metal complexes. *Polyhedron* 1992;11:285—321.
8. Tajmir-Riahi HA. Coordination chemistry of vitamin C. Part I. Interaction of L-ascorbic acid with alkaline earth metal ions in the crystalline solid and aqueous solution. *J Inorg Biochem* 1990;40:181—8.
9. Pizzicannella J, Fonticoli L, Guarnieri S, et al. Antioxidant ascorbic acid modulates NLRP3 inflammasome in LPS-G treated oral stem cells through NF_kB/caspase-1/IL-1β pathway. *Antioxidants* 2021;10:797.
10. Golonka I, Oleksy M, Junka A, Matera-Witkiewicz A, Bartoszewicz M, Musiał W. Selected physicochemical and biological properties of ethyl ascorbic acid compared to ascorbic acid. *Biol Pharm Bull* 2017;40:1199—206.
11. Puente V, Demaria A, Frank FM, Batlle A, Lombardo ME. Antiparasitic effect of vitamin C alone and in combination with benznidazole against *Trypanosoma cruzi*. *PLoS Neglected Trop Dis* 2018;12:e0006764.
12. Langenbach F, Handschel J. Effects of dexamethasone, ascorbic acid and β-glycerophosphate on the osteogenic differentiation of stem cells in vitro. *Stem Cell Res Ther* 2013;4:117.
13. Mizuno M, Fujisawa R, Kuboki Y. Type I collagen-induced osteoblastic differentiation of bone-marrow cells mediated by collagen-α2β1 integrin interaction. *J Cell Physiol* 2000;184:207—13.
14. International organization for standardization. *Dentistry — root canal sealing materials*. Geneva: ISO, 2012. ISO 6876:2012.
15. International organization for standardization. *ISO 9917-1:2007. Dentistry — water-based cements — part 1: powder-liquid acid-base cements*. Geneva: ISO, 2007.
16. International organization for standardization. *ISO 10993-5:2022. Biological evaluation of medical devices — part 5: tests for in vitro cytotoxicity*. Geneva: ISO, 2022.
17. An SY, Lee MJ, Shim YS. X-ray diffraction analysis of various calcium silicate-based materials. *J Dent Hyg Sci* 2022;22:191—8.
18. Taylor HFW. *Cement chemistry*, 2nd ed. London: Thomas Telford, 1997.
19. Zhang L, Yamauchi K, Li Z, Zhang X, Ma H, Ge S. Novel understanding of calcium silicate hydrate from dilute hydration. *Cement Concr Res* 2017;99:95—105.
20. Camilleri J. *Mineral trioxide aggregate in dentistry: from preparation to application*. Berlin: Springer, 2014.
21. Richardson IG. The calcium silicate hydrates. *Cement Concr Res* 2008;38:137—58.
22. Hewlett P, Liska M. *Lea's chemistry of cement and concrete*, 5th ed. Oxford: Butterworth-Heinemann, 2019.
23. Voicu G, Popa AM, Badanoiu AI, Iordache F. Influence of thermal treatment conditions on the properties of dental silicate cements. *Molecules* 2016;21:220.
24. Kravchenko V, Baglyuk G, Trotsan A. Effectiveness of jet milling for producing superfine powders from blast-furnace slag. *Powder Metall Met Ceram* 2017;55:745—50.
25. Ranjan S, Ranjan DM. To evaluate the flowability of various root canal sealers under ISO standardisation — an in vitro study. *Int J Dent Oral Sci* 2021;8:3263—7.
26. Joshi S, Harle SM. Linear variable differential transducer (LVDT) and its applications in civil engineering. *Int J Transp Eng Technol* 2017;3:62—7.
27. Thalacker C. Dental adhesion with resin composites: a review and clinical tips for best practice. *Br Dent J* 2022;232:615—9.
28. Asgary S, Aram M, Fazlyab M. Comprehensive review of composition, properties, clinical applications, and future perspectives of calcium-enriched mixture (CEM) cement: a systematic analysis. *Biomed Eng Online* 2024;23:96.
29. Park YJ, Kang JH, Song HJ, Park YJ. Effect of compositional variation of dental MTA cements on setting time. *J Korean Acad Dent Mater* 2021;48:99—118.
30. Bernardi AV, Souza MT, Montedo ORK, Domingues FHF, Arcaro S, Kopper PMP. Impact of particle size on the setting behavior of tricalcium silicate: a comparative study using ISO 6876 indentation testing and isothermal induction calorimetry. *Bioengineering (Basel)* 2023;11:36.
31. Pires MD, Cordeiro J, Vasconcelos I, et al. Effect of different manipulations on the physical, chemical and microstructural characteristics of biodentine. *Dent Mater* 2021;37:e399—406.
32. Peters OA, Peters CI, Basrani B. Cleaning and shaping of the root canal system. In: Hargreaves KM, Berman LH, eds. *Cohen's pathways of the pulp*, 12th ed. St. Louis: Elsevier, 2020:236—303.
33. Jang GY, Park SJ, Heo SM, Yu MK, Lee KW, Min KS. Washout resistance of fast-setting pozzolan cement under various root canal irrigants. *Restor Dent Endod* 2013;38:248—52.
34. Wu M, Tao B, Wang T, Zhang Y, Wei W, Wang C. Fast-setting and anti-washout tricalcium silicate/disodium hydrogen phosphate composite cement for dental application. *Ceram Int* 2019;45:24182—92.
35. Jang JH, Lee CO, Kim HJ, Kim SG, Lee SW, Kim SY. Enhancing effect of elastinlike polypeptide-based matrix on the physical properties of mineral trioxide aggregate. *J Endod* 2018;44:1702—8.
36. US Army Corps of Engineers. *CRD-C 661-06: specification for antiwashout admixtures for concrete. Vicksburg*. US Army Engineer Research and Development Center, 2006.
37. Bundy KJ, Roberts OC, O'Connor K, McLeod V. Quantification of fibroblast adhesion to biomaterials using a fluid mechanics approach. *J Mater Sci Mater Med* 1994;5:500—2.
38. Hallab NJ, Bundy KJ, O'Connor K, Clark R, Moses RL. Cell adhesion to biomaterials: correlations between surface charge, surface roughness, adsorbed protein, and cell morphology. *J Long Term Eff Med Implants* 1995;5:209—31.
39. Shen C, Rawls HR, Esquivel-Upshaw JF. *Phillips' science of dental materials*, 13th ed. St. Louis: Elsevier Health Sciences, 2021.
40. Bernard M, Jubeli E, Pungente MD, Yagoubi N. Biocompatibility of polymer-based biomaterials and medical devices — regulations, in vitro screening and risk-management. *Biomater Sci* 2018;6:2025—53.